Hydrogen Bonding, Miscibility, Crystallization, and Thermal Stability in Blends of Biodegradable Polyhydroxyalkanoates and Polar Small Molecules of 4-*tert*-Butylphenol

Cheng Chen,[1,2] Peter H. F. Yu,[1] Man Ken Cheung[1]

[1]*Open Laboratory of Chirotechnology, Institute of Molecular Technology for Drug Discovery and Synthesis, Department of Applied Biology and Chemical Technology, Hong Kong Polytechnic University, Hong Kong, People's Republic of China*
[2]*Changchun Institute of Applied Chemistry, Chinese Academy of Sciences, Changchun 130022, People's Republic of China*

Received 20 August 2004; accepted 6 February 2005
DOI 10.1002/app.22082
Published online in Wiley InterScience (www.interscience.wiley.com).

ABSTRACT: The hydrogen bonding, miscibility, crystallization, and thermal stability of poly(3-hydroxybutyrate) (PHB)/4-*tert*-butylphenol (BOH) blends and poly(3-hydroxybutyrate-*co*-3-hydroxyhexanoate) [P(3HB-3HHx)]/BOH blends were investigated by Fourier transform infrared (FTIR) spectroscopy, solid-state ^{13}C-NMR, differential scanning calorimetry, wide-angle X-ray diffraction (WAXD), and thermogravimetric analysis. The results of FTIR spectroscopy and solid-state ^{13}C-NMR show that intermolecular hydrogen bonds existed between the two components in the blends and that the interaction was caused by the carbonyl groups in the amorphous phase of both polyesters and the hydroxyl groups of BOH. With increasing BOH content, the chain mobility of both the PHB and P(3HB-3HHx) components was improved. After the samples were quenched, the detected single glass-transition temperatures decreased with composition, indicating that both PHB/BOH and P(3HB-3HHx)/BOH were miscible blends in the melt. Moreover, as BOH content increased, the melting temperatures of PHB and P(3HB-3HHx) clearly decreased, which implied that their crystallization was suppressed by the addition of BOH. Although the crystallinity of PHB and P(3HB-3HHx) components decreased with increasing BOH content in the blends, their crystal structures were hardly affected after they were blended with BOH, which was further proven by WAXD results. In addition, the thermal stability of PHB was improved by a smaller amount of BOH. © 2005 Wiley Periodicals, Inc. J Appl Polym Sci 98: 736–745, 2005

Key words: crystallization; miscibility; blends

INTRODUCTION

During the past decades, increases in ecological awareness have led to the development of new biodegradable materials that are valid alternatives in specific situations when recycling or incineration is difficult or not economically feasible. Among these biomaterials, microbial polyhydroxyalkanoates (PHAs) are a family of optically active biological polyesters with (R)-3-hydroxyalkanoate [(*R*)-3HA] monomer units that are synthesized by many strains of bacteria as an intracellular storage material of carbon and energy.[1] Because they are produced from renewable resources and are biodegradable to carbon dioxide and water, PHAs are often described as environmentally friendly plastics. So far PHAs have attracted industrial attention as environmentally degradable materials for a wide range of agricultural, marine, and medical applications.[2] The commercially used members of the PHA family are poly(3-hydroxybutyrate) (PHB) and its copolymer poly(3-hydroxybutyrate-*co*-3-hydroxyvalerate) [P(3HB-3HV)]. However, practical application of PHB has often been limited by its brittleness and thermal instability.[3] P(3HB-3HV) is a relatively unusual copolymer because its 3-hydroxybutyrate (3HB) and 3-hydroxyvalerate (3HV) units are isodimorphic; that is, there is similarity in shape and size between these two units.[4] Hence, the usual benefits of the copolymer are not realized for P(3HB-3HV) because of its isodimorphism. To obtain new PHAs with promising properties, a random copolyester, poly(3-hydroxybutyrate-*co*-3-hydroxyhexanoate) [P(3HB-3HHx)], was produced by fermentation with advanced recombinant biotechnology.[5] P(3HB-3HHx) has longer side chains on the backbone than P(3HB-3HV). The X-ray

Correspondence to: M. K. Cheung (bckcheung@inet.polyu.edu.hk).

Contract grant sponsor: Hong Kong Research Grant Council; contract grant number: PolyU 5299/01P.

Contract grant sponsor: University Grants Committee Area of Excellence Scheme (Hong Kong); contract grant number: AoE/P-10/01.

crystallinity of P(3HB-3HHx) decreases from 60 to 18% as the 3HHx fraction increases from 0 to 25 mol %. The tensile strength of the solution-cast films decreases from 43 to 20 MPa as the 3HHx fraction increases from 0 to 17 mol %, and the elongation at break increases from 6 to 850%.[6] Therefore, P(3HB-3HHx) films are relatively softer and more flexible than those of PHB.

Polymer blends have been of great interest to materials scientists because these blends possess improved and modified properties over the individual constituent polymers. Various polymers are blended with PHAs to improve their properties, especially for PHB. These blends include partially biodegradable blends with poly(vinyl acetate)[7] and poly(methyl methacrylate)[8] and completely biodegradable blends with poly(ethylene oxide),[9] poly(vinyl alcohol),[10] polylactide (PLA),[11] poly(ε-caprolactone) (PCL),[12] and polysaccharides.[13] The blending of PHAs and other polymers not only decreases melting point and crystallinity but also reduces cost. Blending has become a convenient way to obtain new materials with promising properties suitable for various end-use purposes.

So far, most components in blends containing PHAs are polymers or macromolecules whose molecular weights are several thousand or above, for example, PHB/PCL[12] and PHB/poly(*p*-vinylphenol).[14] However, studies have seldom examined blends consisting of biodegradable polyesters and small molecules whose molecular weights are below 1000, although this is also an important part of understanding miscible mechanisms and the relationship of miscibility and chain mobility. Generally, small molecules are added into polymers during industrial processing. These act as additives, such as fillers, antioxidants, and plasticizers, to improve the thermal stability and rheology of the polymers. Martin[15] found that poly(ethylene glycol) with a lower molecular weight of 400 was a good plasticizer of PLA. The addition of poly(ethylene glycol) significantly decreased the glass-transition temperature (T_g) of PLA and obviously improved the mechanical properties of blends containing PLA and thermoplastic starch. Zhu and coworkers[16,17] investigated binary blends of catechin and polyesters, including PCL, poly(L-lactide) (PLLA), poly(D-lactide) (PDLA), poly(D,L-lactide) (PDLLA), and poly(3-hydroxypropionate), and the results showed that no intermolecular hydrogen bonds existed between the PLAs and catechin at room temperature, unlike the blend of poly(3-hydroxypropionate) and catechin. However, weak hydrogen bonds were found in the quenched PLA/catechin blends. For PLLA, PDLA, and PDLLA, the steric hindrance of the methyl groups on the side chains might have restrained the formation of hydrogen bonds. These authors also investigated the formation of the interassociated hydrogen bonds between PCL and 4,4′-thiodiphenol (TDP) as a function of composition and temperature. They found that TDP molecules influenced the molecular motion of PCL, mainly by lowering its crystallinity rather than by forming a hydrogen-bonded network with PCL chains.[18–20] Therefore, the effect of polar small molecules on polymers is an interesting topic, especially in biodegradable polyester. If one investigates the blends based on biodegradable polyesters and polar small molecules, the relation of miscibility and chain mobility can be further understood. At the same time, the effect of polar small molecules on polymer morphology and properties can be also revealed, which may serve as a guide during practical processing.

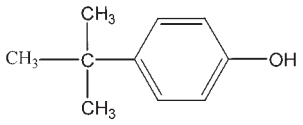

Figure 1 Chemical structure of BOH.

As one of a series of studies of the blends of biodegradable PHAs and polar small molecules, this study examined two systems: PHB/4-*tert*-butylphenol (BOH) blends and P(3HB-3HHx)/BOH blends. In this study, the intermolecular hydrogen bonding, miscibility, crystallization, and thermal stability of the two blend systems were investigated by FTIR spectroscopy, solid-state ^{13}C-NMR, differential scanning calorimetry (DSC), wide-angle X-ray diffraction, and thermogravimetric analysis (TGA). The effects of differences in the side-chain length of PHB and P(3HB-3HHx) on the chain mobility and formation of intermolecular hydrogen bonds were also studied.

EXPERIMENTAL

Materials

PHB was purchased from Aldrich (St. Louis, MO), and its weight-average molecular weight (M_w) was 400–700 kDa according to the supplier. P(3HB-3HHx) was biosynthesized at Tsinghua University in Beijing, China, with bacteria strain *Pseudomonas stutzeri* 1371 in a glucose mineral-salt medium. The molar ratio 3HB/3-hydroxyhexanoate (3HHx) (85:15) was determined with a gas chromatography procedure, which involved dissolution of the P(3HB-3HHx) in an esterification liquid mixture.[21] M_w of P(3HB-3HHx) was about 750 kDa. BOH of chemical purity was purchased from Shanghai Chemical Reagent Co., Ltd. (Shanghai, China). BOH was purified by the recrystallization method before use. Its chemical structure is shown in Figure 1. The other reagents were used as received.

Preparation of samples

The blends of PHB and P(3HB-3HHx) with BOH were prepared by the dissolution of both polymers and

BOH in chloroform ($CHCl_3$). The solutions were cast onto Petri dishes and evaporated at room temperature to remove the solvent. Finally, the blends were dried *in vacuo* at 40°C for 24 h and then kept in a desiccator. Because the materials were of little practical use when the BOH content was above 50%, various blends were prepared, as mentioned previously, with weight ratios ranging from 90/10 to 50/50, with the latter number referring to the BOH percentage.

Measurements

A PerkinElmer DSC-7 differential scanning calorimeter (PerkinElmer, Boston, MA) was used to study glass-transition temperature (T_g), crystallization, and melting behavior of the PHB/BOH blends and P(3HB-3HHx)/BOH blends. The temperature and energy readings of the instrument were calibrated with indium in the measurements. The specimens were packed in aluminum pans and heated from −50 to 190°C (run I) at a heating rate of 10°C/min under a nitrogen atmosphere. The specimens were maintained at 190°C for 2 min to destroy any residual nuclei before they were rapidly quenched to −50°C. The specimens were reheated to 190°C at a heating rate of 10°C/min (run II). The value of the midpoint of the transition was taken as the T_g. The melting temperature (T_m) and cold crystallization temperature (T_{cc}) were taken as the peak values of the respective endothermal and exothermal processes in the DSC curves.

Fourier transform infrared (FTIR) spectra were recorded on a Nicolet Avatar 360 FTIR spectroscope (Pittsfield, MA). All spectra were recorded at room temperature with 32 scans at a resolution of 4 cm^{-1}. Thin films of the samples were cast from the $CHCl_3$ solution onto KBr pellets. The films were dried at room temperature until $CHCl_3$ was completely removed.

High-resolution, solid-state NMR experiments were carried out at ambient temperature (27°C) on a Varian Inova high-power, wide-bore, 400-MHz NMR spectrometer (Varian Inova, Palo Alto, CA) at resonance frequencies of 399.7 MHz for ^1H and 100.5 MHz for ^{13}C. The samples were placed into 7.5-mm Chemagnetics pencil rotors. High-resolution, solid-state ^{13}C-NMR spectra were obtained with the technique of a ^{13}C single pulse with ^1H decoupling and magic-angle spinning (DD/MAS). The predelay recycle time was 25.0 s.

WAXD experiments were performed with a Philips PW 1700 X-ray diffractometer (The Netherlands) with Cu Kα X-rays with a voltage of 30 kV and a current of 20 mA. The samples for WAXD analysis were prepared by a solution-casting method and isothermal treatment at 40°C for 48 h for full crystallization.

The thermal stability of the samples was investigated in the temperature range 25–600°C with the PerkinElmer TGA 7 apparatus in a nitrogen atmosphere. The experiments were carried out at a heating rate of 20°C/min with 10-mg samples.

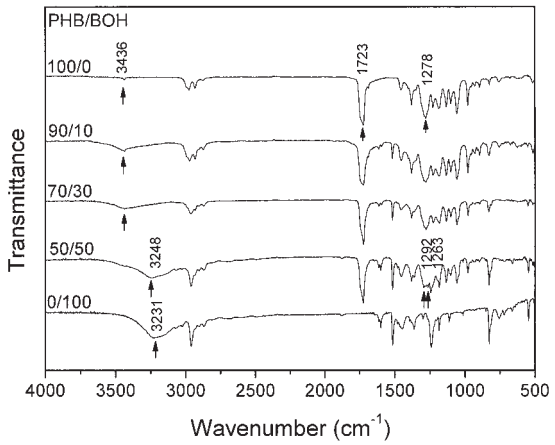

Figure 2 FTIR spectra of PHB, BOH, and PHB/BOH blends with different compositions.

RESULTS AND DISCUSSION

Hydrogen bonds of both blend systems

As shown in Figure 1, BOH has a phenol hydroxyl group. Hence, we speculated that BOH could form hydrogen bonds with PHB and P(3HB-3HHx) in the blends because BOH is a proton-donating component and both PHB and P(3HB-3HHx) are proton-accepting components. To detect the existence of hydrogen bonds in the blends, FTIR was used because it is the most common technique for studying intermolecular and intramolecular interactions in polymer blends and complexes. Changes in the intensity and position of the FTIR peaks resulting from some characteristic functional groups could be attributed to the existence of the intermolecular interactions.

Figure 2 shows the FTIR spectra of PHB, BOH, and PHB/BOH blends. There was a strong and sharp transmittance band at 1723 cm^{-1} in the spectrum of pure PHB, which was attributed to the stretching vibrations of crystalline carbonyl groups. The band at 3436 cm^{-1}, attributed to PHB's hydroxyl end groups, was very weak. The amorphous carbonyl vibration of PHB at 1740 cm^{-1} was not clearly observed in the spectrum.[22] In the spectrum of pure BOH, the band at 3231 cm^{-1} was strong and broad, and this was attributed to the phenol hydroxyl stretching vibration. The peak was related to hydrogen bonds among the BOH molecules. Because BOH molecules can form hydrogen bonding among themselves, the wave number of hydrogen-bonded phenol hydroxyl groups is obviously smaller than those of free hydroxyl groups (>3600 cm^{-1}) and the hydroxyl groups of dimer hydrogen bonds (3400–3500 cm^{-1}).

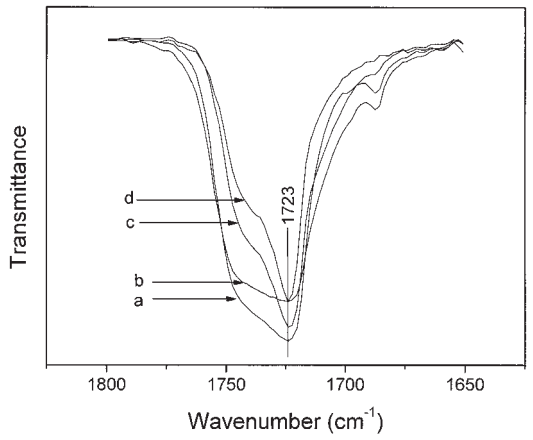

Figure 3 FTIR spectra of PHB and PHB/BOH blends with different compositions in the carbonyl region: (a) pure PHB and (b) 90/10, (c) 70/30, and (d) 50/50 PHB/BOH.

For PHB/BOH blends with compositions of 90/10 and 70/30, the band of the PHB component at 3436 cm^{-1} became obviously stronger, although its position hardly shifted. Because there were very few hydroxyl end groups in the PHB component, its contribution to the 3436-cm^{-1} peak may have been negligible, so the change in the intensity of the band at 3436 cm^{-1} may have mainly originated from BOH. As the BOH content in the blends reached 50%, the hydroxyl band shifted, and its wave number decreased from 3436 to 3248 cm^{-1}. This result suggests that the hydroxyl groups of BOH molecules took part in the formation of intermolecular hydrogen bonds with the carbonyl groups of PHB, causing its wave number to decrease. Moreover, the intensity of the band at 3248 cm^{-1} was also relatively stronger, which implied that the amount of BOH causing intermolecular interaction increased. Because the wave number of the phenol hydroxyl groups in pure BOH was lower, the intermolecular hydrogen bonds between the PHB and BOH components were relatively weaker than those of pure BOH. As shown in Figure 2, with increasing BOH content, the intensity of the band at 1278 cm^{-1} gradually weakened. When the BOH content was 50%, the band at 1278 cm^{-1} disappeared, and two new bands were observed in the spectrum at 1292 and 1263 cm^{-1}. The bands at 1278 cm^{-1} were crystalline sensitive. In the spectrum of crystalline PHB, the band at 1278 cm^{-1} was noticeably present, although it was not present in the spectrum of amorphous PHB.[23] The result suggests that the hydrogen bonds existing in the blends suppressed the crystallization of the PHB component.

Figure 3 shows the FTIR spectra of PHB and the PHB/BOH blends with different compositions in the carbonyl region. Their peak width clearly decreased as BOH content increased. The crystalline carbonyl peak of the PHB component still remained at 1723 cm^{-1}, the same as that of pure PHB. However, the intensity at about 1723 cm^{-1} gradually increased relative to that of the amorphous carbonyl band at 1740 cm^{-1}. The amorphous carbonyl peak shifted slightly to a lower wave number. This suggested that intermolecular hydrogen bonding took place in the amorphous region of the carbonyl groups rather than in the crystalline carbonyl groups at 1723 cm^{-1} because, as discussed above, the intensity of the crystalline-sensitive band at 1278 cm^{-1} decreased with increasing BOH content.

Figure 4 shows the FTIR spectra of P(3HB-3HHx), BOH, and P(3HB-3HHx)/BOH blends with different compositions in the hydroxyl region. For P(3HB-3HHx), no clear hydroxyl transmittance was observed in this region. Consequently, any changes in the region were directly attributed to changes such as intermolecular interaction in the environments of the BOH hydroxyl groups. In the FTIR spectra of the P(3HB-3HHx)/BOH blends, a new broad band was evident in the hydroxyl region, and its position shifted to lower wave numbers as the BOH content increased. When the BOH content increased from 10 to 50%, the position of the band dropped from 3469 to 3445 cm^{-1}, and the value of its wave number decreased about 24 cm^{-1}. This was a result of intermolecular hydrogen bonds, which were caused by the hydroxyl groups of the BOH component and the carbonyl groups of the P(3HB-3HHx) component. By comparing the position of the hydrogen-bonded hydroxyl band in both blend systems of the same composition, we found that PHB (3436–3248 cm^{-1}) could form stronger hydrogen bonds with BOH than could P(3HB-3HHx) (3469–3445 cm^{-1}). Presumably, this was induced by the steric hindrance effect of the longer side chains in P(3HB-3HHx). For PHAs, longer side chains might hinder,

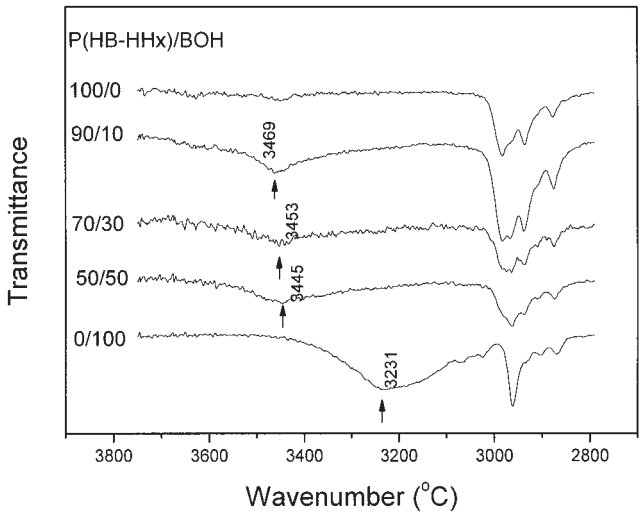

Figure 4 FTIR spectra of P(3HB-3HHx), BOH, and P(3HB-3HHx)/BOH blends with different compositions in the hydroxyl region.

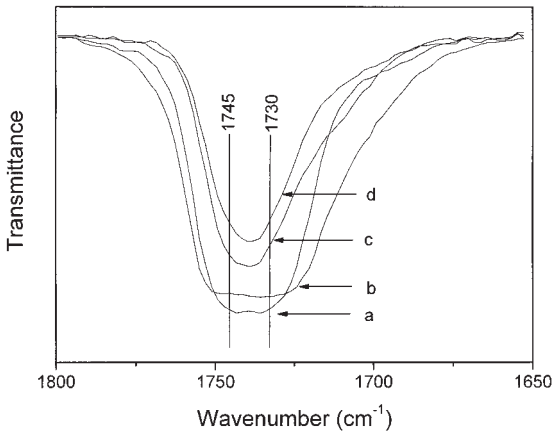

Figure 5 FTIR spectra of P(3HB-3HHx) and P(3HB-3HHx)/BOH blends with different compositions in the carbonyl region: (a) pure P(3HB-3HHx) and (b) 90/10,(c) 70/30, and (d) 50/50 P(3HB-3HHx)/BOH.

not restrain, the formation of intermolecular hydrogen bonds. This result was different from that of a previous report.[16]

Figure 5 shows the FTIR spectra of the P(3HB-3HHx) and P(3HB-3HHx)/BOH blends with different compositions in the carbonyl region. BOH showed no transmittance in this region. For pure P(3HB-3HHx), a strong and broad carbonyl band was evident in the region, which consisted of crystalline (1730 cm^{-1}) and amorphous (1745 cm^{-1}) stretching vibrations. However, for P(3HB-3HHx)/BOH blends, the band gradually became sharper as BOH content increased. As BOH content in the blends rose above 30%, the band focused on the position of 1737 cm^{-1}. The absence of a crystalline carbonyl peak after blending with BOH might be explained by suppression of its crystallization. At the same time, the amorphous carbonyl groups participate in intermolecular hydrogen bonding, causing the wave number of the amorphous carbonyl band to decrease from 1745 to 1737 cm^{-1}. For both blend systems, no new bands caused by intermolecular hydrogen bonds were observed at lower wave numbers, indicating that intermolecular hydrogen bonds between the two components were weak.

High-resolution, solid state ^{13}C-NMR is another powerful tool for investigating intermolecular hydrogen bonds. In general, hydrogen bonds can result in chemical shifts of the carbonyl resonance and the hydroxyl resonance. In blends of PCL and TDP, a significant downfield shift of about 2 ppm was observed for the carbonyl resonance.[24] DD/MAS ^{13}C-NMR spectra of the PHB/BOH and P(3HB-3HHx)/BOH blends with different compositions are shown in Figure 6(a,b). Assignments and chemical shifts of PHB, P(3HB-3HHx), and BOH are also shown in Figure 6 and Table I. The small peaks with a star symbol were from the Teflon background of the probe.

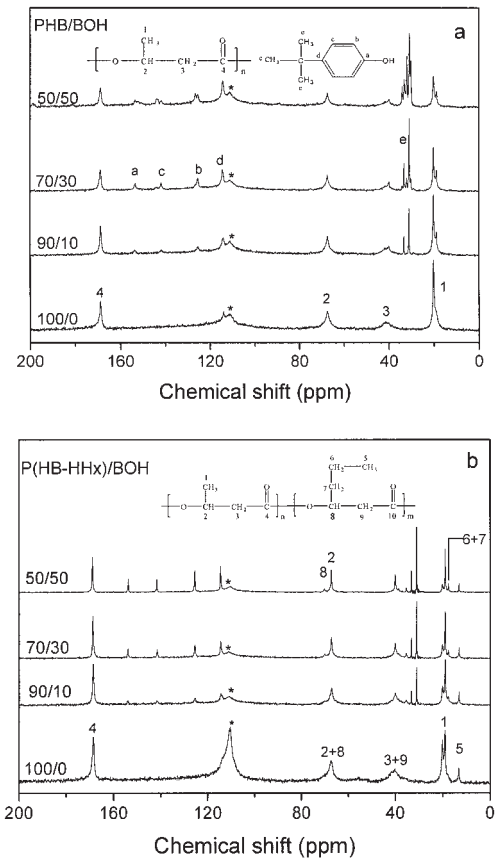

Figure 6 DD/MAS ^{13}C-NMR spectra of (a) PHB/BOH blends and (b) P(3HB-3HHx)/BOH blends with different compositions.

After blending with BOH, the chemical shifts of the PHB and P(3HB-3HHx) components were hardly affected. The largest observed shift was the carbonyl resonance of P(3HB-3HHx), which was only 0.5 ppm. However, the line shape of the DD/MAS NMR resonances for the PHB and P(3HB-3HHx) components was obviously changed, especially for the P(3HB-3HHx) component. As seen in Figure 6, many overlapped peaks were clear in the spectra with increasing BOH content, for example, for the methine groups of P(3HB-3HHx) [Fig. 6(b)]. Table II shows the line width of the methine resonance in both blends systems. The

TABLE I
Chemical Shifts of PHB, P(3HB-3HHx), and BOH Components in the Blends with Different Compositions

	PHB/BOH (ppm)		P(3HB-3HHx)/BOH (ppm)	
Sample	C═O	C—OH	C═O	C—OH
100/0	168.7	—	168.5	—
90/10	168.8	153.6	168.7	154.1
70/30	168.9	153.5	168.8	154.0
50/50	168.9	153.5	169.0	153.8

TABLE II
Line Width (Hz) of Backbone Methine Resonance for PHB/BOH Blends and P(3HB-3HHx)/BOH with Different Compositions

	CH (at 67.4 ppm)	
Sample	PHB/BOH	P(3HB-3HHx)/BOH
100/0	216.0	220.1
90/10	179.4	143.0
70/30	144.1	69.9
50/50	161.7	41.9

Line broadening = 1 Hz.

line width of the methine resonance in both blend systems decreased remarkably with increasing BOH composition. When the BOH content was above 30% in the P(3HB-3HHx)/BOH blends, the solid-state ^{13}C-NMR spectra showed some characteristics of liquid NMR spectra. The smaller the values of the line width were, the more flexible the molecular chains were. Hence, the results indicate that the chain mobility of both polyesters in the blends was improved.

In addition, the DD/MAS NMR resonances of each of the methyl groups in PHB and P(3HB-3HHx) components were split into two peaks (Fig. 7): the one at 20.2 ppm was attributed to crystalline methyl groups; the other at 19.0 ppm was attributed to amorphous methyl groups. With increasing BOH content, the relative intensity of amorphous methyl groups increased significantly, whereas that of the crystalline methyl groups decreased remarkably. This was more obvious in the P(3HB-3HHx)/BOH blends. The results imply that the crystallinity of the PHB and P(3HB-3HHx) components decreased with increasing BOH content and that intermolecular hydrogen bonds seriously

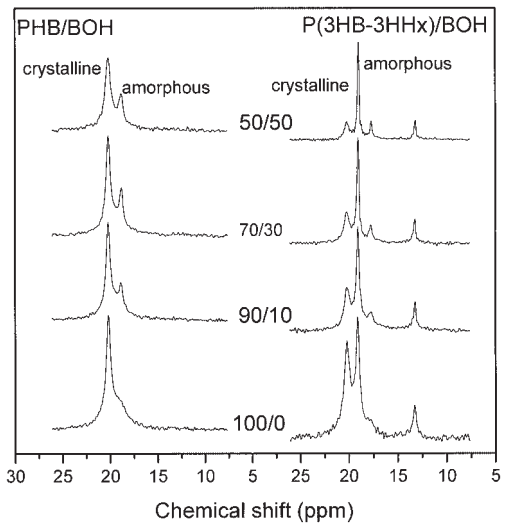

Figure 7 Methyl resonance in the ^{13}C-NMR DD/MAS spectra of PHB/BOH blends and P(3HB-3HHx)/BOH blends with different compositions.

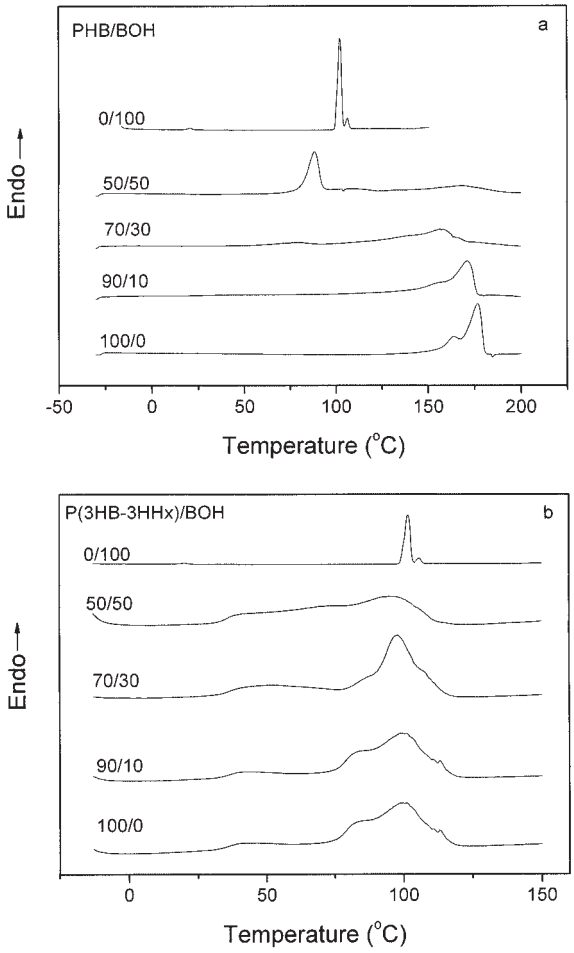

Figure 8 DSC curves of (a) PHB/BOH blends and (b) P(3HB-3HHx)/BOH blends during the first heating run.

hindered the crystallization of the polymers. In the spectra of the P(3HB-3HHx)/BOH blends, a new peak at 17.7 ppm, attributed to the methylene groups of the 3HHx unit, was observed (Fig. 7). This was another indication that chain mobility improved, so the fine resonance was detected.

Miscibility of both blend systems

It is well known that T_g of polymer blends is one of the most important criteria in the miscibility of the components. For binary blends, if the components are miscible at the level 5–10 nm in the main chain, usually only one T_g will appear in DSC thermograms at an intermediate temperature compared to that of the T_g value of each pure polymer.[25] Therefore, thermal characterization of polymer blends is necessary to determine their miscibility.

Figure 8(a,b) shows the DSC curves of the PHB/BOH and P(3HB-3HHx)/BOH blends with different compositions during the first heating run. The DSC curves of pure PHB and pure P(3HB-3HHx) exhibited

double melting peaks, which resulted from the preparation of samples and heat treatment. The melting peak at the lower temperature was attributed to the melting of the cast crystalline film. An exothermal peak arising from dynamic recrystallization during the heating should have existed between the two endothermal peaks. Another endothermal peak appearing at the higher temperature was attributed to the melting of the recrystallized component.[26] Hence, it was reasonable that the lower endothermal peak was the actual T_m of the cast films. A broad melting shoulder was observed between 60 and 80°C in the DSC curves of pure P(3HB-3HHx), which reflected its premelting behavior.[27] Premelting corresponds to an intermediate state between the ordered crystalline and amorphous states.[27] In addition, no obvious glass transition was observed in any of the DSC heating curves, presumably because of high crystallinity that rendered detection difficult. BOH appeared as a white crystal powder, and its DSC curve also exhibited two melting peaks. The strong melting peak at the lower temperature of about 101.8°C was its T_m; the other weak peak was attributed to the melting of recrystallization resulting from the imperfect crystals of BOH.

As seen in Figure 8(a), the T_m's of the PHB/BOH blends gradually decreased as BOH content in the blends increased, and their melting enthalpies (ΔH_m) clearly fell. Table III lists the T_m's and melting enthalpies of the PHB/BOH and P(3HB-3HHx)/BOH blends in run I. T_m of pure PHB was about 176.8°C. When the BOH content in the blends increased from 10 to 30%, T_m's of the PHB component decreased from 171.3 to 156.5°C. Meanwhile, the melting enthalpy of the PHB component decreased from 77.7 to 48.5 J/g. When the BOH content was 30%, only the melting peak of PHB was shown in the DSC curve, indicating that BOH was dispersed into the polyester and was hardly crystallized. As the BOH content increased to 50%, the melting peak of the PHB component almost disappeared, and a melting peak attributable to the melting of BOH crystals was observed at 88.4°C; some crystalline BOH could be seen on the surface of the cast film, implying that excess BOH molecules were excluded from the polymer. The intermolecular hydrogen bonds not only suppressed the crystallization of the polyester but also hindered the crystallization of BOH.

Meanwhile, T_m's of the P(3HB-3HHx)/BOH blends decreased slightly as BOH content increased [Fig. 8(b)], compared with those of the PHB/BOH blends with the same compositions. When the BOH content was increased from 0 to 50%, T_m's of P(3HB-3HHx) decline only from 102.3 to 95.5°C (as shown in Table III). In addition, no melting peak attributable to BOH was observed in any of the DSC curves of the P(3HB-3HHx)/BOH blends, even when the BOH content in the blends was 50%. This further supported the suggestion that because of its lower crystallinity, P(3HB-3HHx) formed more hydrogen bonds with BOH than PHB, although these bonds may have been weaker.

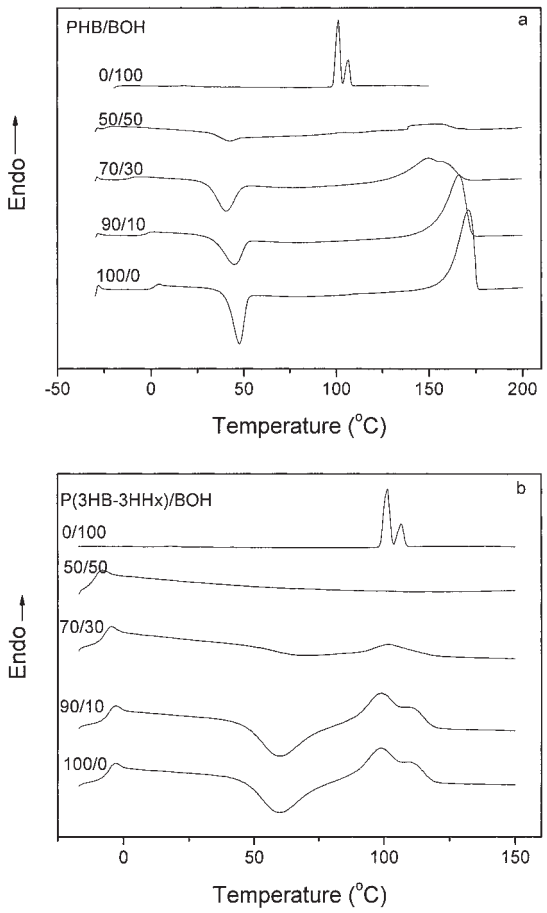

Figure 9 DSC curves of (a) PHB/BOH blends and (b) P(3HB-3HHx)/BOH blends during the second heating run.

After the first heating, the samples were quenched to −50°C and heated again to 190°C for the second run. The DSC results for run II show that the T_g values in both blend systems clearly decreased with BOH content [as shown in Fig. 9(a,b) and Table III]. This means that both blend systems were miscible in the melt state. The decrease in T_g indicated an increase in the chain mobility of polymers because the segments of the polymers could be mobile at lower temperatures.[28] This also suggested that the addition of BOH remarkably improved the chain mobility of the polyesters, which is in accordance with the previous solid-state ^{13}C-NMR results. The changes in T_g could be attributed to the formation of intermolecular hydrogen bonds in the blends. Because of the existence of intermolecular hydrogen bonds, BOH might have been physically grafted onto the chains of the polyesters. Moreover, its great steric effect favored the separation of the twisted chains of the polymers. Hence, BOH was dispersed into the polyesters after it was blended with polymers and acted as a plasticizer by increasing the flexibility of the PHB and P(3HB-3HHx) chains, as observed by the decrease in T_g.

TABLE III
DSC Data of PHB/BOH Blends and P(3HB-3HHx)/BOH Blends with Different Compositions

Sample	Run I		Run II			
	T_m (°C)	ΔH_m (J/g)	T_g (°C)	T_{cc} (°C)	T_m (°C)	ΔH_m (J/g)
PHB	176.8	81.7	1.2	47.5	171.2	80.2
PHB/BOH 9/1	171.3	77.7	−2.7	44.9	166.0	79.9
PHB/BOH 7/3	156.5	48.5	−11.6	40.5	149.9	53.3
PHB/BOH 5/5	88.4	44.7	−23.2	42.0	—	—
P(3HB-3HHx)	102.3	35.4	−4.1	66.0	103.9	18.0
P(3HB-3HHx)/BOH 9/1	99.6	31.4	−6.6	59.5	99.0	12.4
P(3HB-3HHx)/BOH 7/3	97.8	24.2	−8.2	—	100.3	3.6
P(3HB-3HHx)/BOH 5/5	95.5	9.9	−11.7	—	—	—

During the second heating run, cold crystallization peaks were observed in the DSC curves of the PHB/BOH and P(3HB-3HHx)/BOH blends, and they gradually shifted to lower temperatures as the BOH content in the blends increased [Fig. 9(a,b) and Table III]. Generally, cold crystallization may have taken place at a high enough temperature above the T_g of the polymer, where the crystallizable polymer chains had enough segmental mobility to crystallize.[29] For the PHB/BOH blends, their T_{cc}'s clearly decreased, whereas T_{cc}'s of the P(3HB-3HHx)/BOH blends decreased slightly. Cold crystallization mainly resulted from the inability of all of the crystallizable chains to crystallize fully during the cooling cycles. The remaining chains could recrystallize again when the segments regained mobility on heating above T_g. Consequently, the decease in T_{cc} could also be explained by consideration of the chain mobility. The addition of BOH improved the flexibility of the PHB and P(3HB-3HHx) components and promoted their chain mobility so that their crystallization could take place at lower temperatures when they were heated from the amorphous state. Thus, the tendency of T_{cc} was similar to that of T_g. However, for the P(3HB-3HHx)/BOH blend with a 70/30 composition, the cold crystallization peak almost disappeared in the DSC curve, which implied that the crystallization of the P(3HB-3HHx) component was almost completed during quenching.

The PHB/BOH and P(3HB-3HHx)/BOH blends showed different melting behavior in run II compared with run I. With increasing BOH content in the blends, the melting peaks of the PHB/BOH blends gradually decreased. Pure PHB and the PHB/BOH blends with a 90/10 composition showed a single melting peak instead of multiple melting peaks in run I, indicating that their crystallization began from a homogeneous phase. When the BOH content reached 30%, the melting curve showed double melting peaks. The melting peak became a wide plateau as the BOH content increased. For the P(3HB-3HHx)/BOH blend with a 90/10 composition, the DSC curve showed double melting peaks. The melting peak at the lower temperature was stronger, whereas the peak at the higher temperature was weaker, which was also the result of recrystallization. When the BOH content in the P(3HB-3HHx)/BOH blends reached 50%, no melting peak was observed [Fig. 9(b)], which corresponded to the absence of cold crystallization during heating. The results imply that the P(3HB-3HHx) blend with a 50/50 composition was completely in an amorphous state. Therefore, blending BOH with PHB and P(3HB-3HHx) not only improved chain flexibility but also changed the semicrystalline polymer into a fully amorphous elastomer when BOH content was high enough. In addition, no melting peak corresponding to the BOH component was detected in any of the DSC melting curves shown in Figure 9. This also supported the view that BOH was miscible with PHB and P(3HB-3HHx) in the melt so that its crystallization was fully suppressed.

Crystallization of both blend systems

To further study the effects of BOH on the PHB and P(3HB-3HHx) components, the crystalline structures of both blend systems were studied by WAXD. The X-ray diffraction patterns of the PHB/BOH and P(3HB-3HHx)/BOH blends are shown in Figure 10(a,b). Although P(3HB-3HHx) is a copolyester containing 3HB and 3HHx units, only one crystalline form of the P(3HB) lattice was observed in the diffraction of P(3HB-3HHx) because of the lower content of the 3HHx unit [Fig. 10(b)]. Hence, the diffraction peaks of pure PHB and pure P(3HB-3HHx) were similar, but the diffraction peaks of pure PHB showed more regularity than that of P(3HB-3HHx). In the diffraction of pure PHB, the diffraction peaks of (021), (101), and (111) were three independent peaks that merged to form a broad peak. They become a broad overlapped peak in the diffraction of pure P(3HB-3HHx). This meant that the PHB crystals were better than those of P(3HB-3HHx). In the diffractions of both blend systems, the diffraction peaks of the PHB and P(3HB-3HHx) components decreased. Their peak width rose as BOH content increased, which meant that the crystallinity of the PHB and P(3HB-3HHx) components

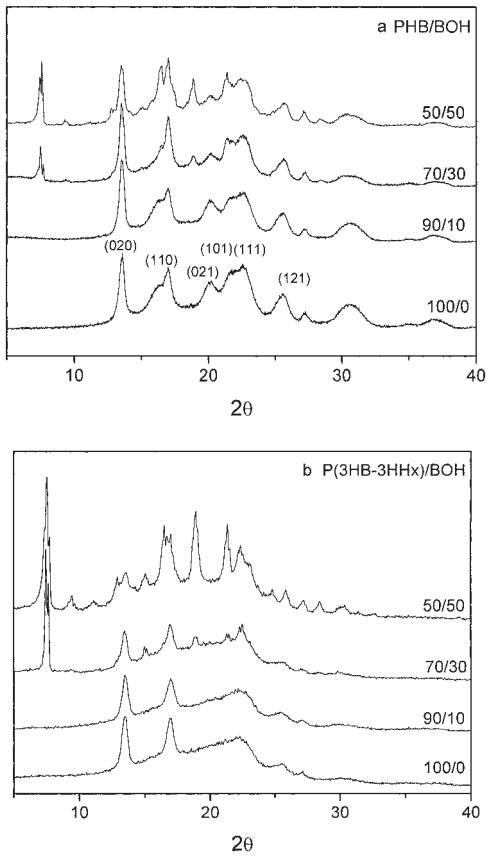

Figure 10 WAXD profiles of (a) PHB/BOH blends and (b) P(3HB-3HHx)/BOH blends with different compositions.

decreased, and their crystal regularity also became weak. However, the *d*-spacing values of the PHB and P(3HB-3HHx) components were constant for all crystallographic planes, which indicated that the PHB and P(3HB-3HHx) unit cells were not changed. In the blends, the BOH molecules were excluded from the crystal lattice of PHB and P(3HB-3HHx), so they remained in the amorphous region. Thus, hydrogen bonding only took place in the amorphous region between the carbonyl groups of the polyesters and the hydroxyl groups of BOH. When the BOH content in the blends was above 30%, the diffraction peaks of the BOH components were observed. When the relative intensities of the diffraction peaks were compared, that of BOH in the P(3HB-3HHx) component was found to be obviously stronger than that in the PHB component, indicating that the crystallization of the P(3HB-3HHx) component was more intensively suppressed by BOH than that of PHB. When the BOH content in the blends reached 50%, the PHB component could still crystallize, whereas the diffraction peaks of the P(3HB-3HHx) component almost disappeared (Fig. 10). The P(3HB-3HHx)/BOH blend with a 50/50 composition became a fully amorphous elastomer, in agreement with the DSC results.

Thermal stability of both blend systems

Figure 11(a,b) shows the TGA curves of the PHB/BOH and P(3HB-3HHx)/BOH blends decomposed in a nitrogen atmosphere. As shown, the weight loss of pure PHB and pure P(3HB-3HHx) occurred in one step in the temperature range from 250 and 320°C, and the thermal stability of pure P(3HB-3HHx) was better than that of pure PHB, as reported in previous study.[30] Their thermal decomposition temperatures at the onset of weight loss (T_{onset}'s) were 266 and 287°C, respectively. For the PHB/BOH and P(3HB-3HHx)/BOH blends, when the BOH content was above 30%, both blend systems showed a two-step process, which resulted from the thermal decomposition of BOH. The addition of BOH slightly improved the thermal stability of the PHB components, especially when the BOH content was lower. With 10% BOH, the PHB/BOH blend showed a one-step process of thermal decomposition, and its T_{onset} was 274°C. Its thermal decomposition temperature increased about 8°C compared to that of pure PHB. However, the thermal decomposition temperatures of the P(3HB-3HHx)/BOH blends

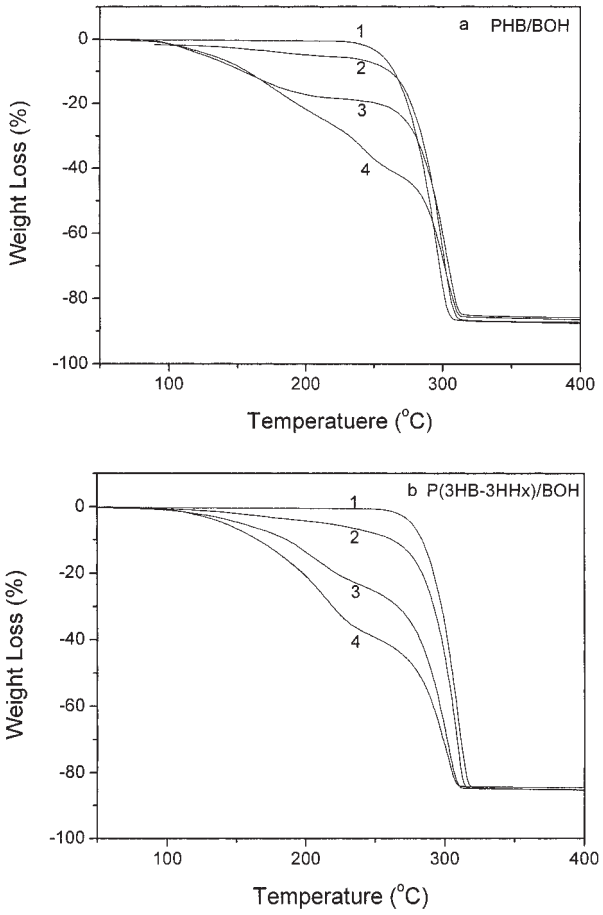

Figure 11 TGA curves of (a) PHB/BOH blends and (b) P(3HB-3HHx)/BOH blends with different compositions decomposed in nitrogen: (1) 100/0, (2) 90/10, (3) 70/30, and (4) 50/50.

were hardly affected by the addition of BOH. In addition, the rate of thermal decomposition was higher for the P(3HB-3HHx) component relative to that of the PHB component because its range of thermal decomposition was narrower. When one considers that thermal decomposition of P(3HB-3HHx) occurred at higher temperatures, the higher temperature was the primary factor resulting in the increase in the thermal decomposition rate of the P(3HB-3HHx) component.

CONCLUSIONS

FTIR results show that there existed intermolecular hydrogen bonds in the PHB/BOH and P(3HB-3HHx)/BOH blends that were mainly between the carbonyl groups in the amorphous phase of the PHB and P(3HB-3HHx) components and the hydroxyl groups of BOH. P(3HB-3HHx) had a lower crystallinity than PHB in the blends and so formed intermolecular hydrogen bonds more easily with BOH. However, the intermolecular interaction between P(3HB-3HHx) and BOH was weaker than that between PHB and BOH because of the steric hindrance of longer 3HHx side chains. In the solid-state ^{13}C-NMR resonances of both blend systems, the resonance shapes of the PHB and P(3HB-3HHx) components became sharper and their line width decreased, which implied that the addition of BOH improved the chain mobility of the polyesters. Single T_g values indicated that both blend systems were miscible in the melt in the investigated composition range. After quenching, T_{cc}, T_m, and the melting enthalpy of the PHB and P(3HB-3HHx) components substantially decreased and approached zero at about 50% BOH, especially for the P(3HB-3HHx) component. This meant that the crystallization of both polyesters was suppressed after blending with BOH. The effect of BOH on PHB and P(3HB-3HHx) was not only to improve their chain flexibility but also to change the semicrystalline polymer in the pure state into a fully amorphous elastomer if the BOH content was high enough. Although the crystallinity of the PHB and P(3HB-3HHx) components decreased after blending with BOH, their crystalline structures were not changed, which was proven by the WAXD results. The TGA results show that P(3HB-3HHx) was more stable in nitrogen than PHB, and a smaller amount of BOH could retard the thermal decomposition of PHB.

The authors thank Qingan Meng for acquiring NMR data.

References

1. Doi, Y. Microbial Polyester; VCH: New York, 1990.
2. Sudesh, K.; Abe, H.; Doi, Y. Prog Polym Sci 2000, 25, 1503.
3. Chiellini, E.; Solaro, R. Adv Mater 1996, 8, 4.
4. Bloembergen, S.; Holden, D. A.; Hamer, G. K. Macromolecules 1986, 19, 2865.
5. Shimamura, E.; Kasuya, K. Macromolecules 1994, 27, 878.
6. Doi, Y.; Kitamura, S.; Abe, H. Macromolecules 1995, 28, 4822.
7. Kumagai, Y.; Doi, Y. Polym Degrad Stab 1992, 35, 87.
8. Lotti, H.; Pizzoli, M.; Ceccorulli, G. Polymer 1993, 34, 4935.
9. Arella, M.; Martuscelli, E.; Rajmo, M. Polymer 1993, 34, 3234.
10. Azuma, Y.; Yoshie, N.; Sakurai, M. Polymer 1992, 33, 4763.
11. Zhang, L. L.; Xiong, C. D.; Deng, X. M. Polymer 1996, 37, 235.
12. Gassner, F.; Owen, A. J. Polymer 1994, 35, 2233.
13. Zhang, L. L.; Deng, X. M.; Zhao, S. J. Polymer 1997, 38, 6001.
14. Xing, P. X.; Dong, L. D.; An, Y. X. Macromolecules 1997, 30, 2726.
15. Martin, O.; Averous, L. Polymer 2001, 42, 6209.
16. Zhu, B.; Li, J. C.; He, Y. J Appl Polym Sci 2004, 91, 3565.
17. Zhu, B.; Li, J. C.; He, Y. Macromol Biosci 2003, 3, 684.
18. Li, J. C.; He, Y.; Inoue, Y. J Appl Polym Sci 2001, 39, 2108.
19. He, Y.; Asakawa, N.; Inoue, Y. J Polym Sci Part B: Polym Phys 2000, 38, 1848.
20. He, Y.; Inoue Y. Biomacromolecules 2003, 4, 1865.
21. Xi, J.; Wu, Q.; Zhuang, Z. Antonie van Leeuwenhoek 2000, 78, 43.
22. Bloembergen, S.; Holden, D. A.; Hamer, G. K. Macromoleculars 1986, 19, 2865.
23. Chen, C.; Fei, B.; Peng, S. W. J Appl Polym Sci 2002, 84, 1789.
24. He, Y.; Asakawa, N.; Inoue, Y. Macromol Chem Phys 2001, 202, 1035.
25. Paul, D. R.; Bucknall, C. B. Polymer Blends; Wiley: New York, 2000; Vol. 1.
26. Pearce, R.; Marchessault, R. H. Polymer 1994, 35, 3990.
27. Wu, Q.; Tian, G.; Sun, S. Q. J Appl Polym Sci 2001, 82, 934.
28. Mandelken, L. Crystallization of Polymers; McGraw Hill: New York, 1964.
29. Xing, P. X.; Ai, X.; Dong, L. S. Macromolecules 1998, 31, 6898.
30. He, J. D.; Cheung, M. K.; Yu, P. H. J Appl Polym Sci 2001, 82, 90.